ARTICLE

Measuring Cell Wall Thickness in Living Yeast Cells Using Single Molecular Rulers

Vincent Dupres,[†,§] Yves F. Dufrêne,[†,§,*] and Jürgen J. Heinisch[‡,*]

[†]Institute of Condensed Matter and Nanosciences, Université catholique de Louvain, Croix du Sud 2/18, B-1348 Louvain-la-Neuve, Belgium, and [‡]Fachbereich Biologie/Chemie, Universität Osnabrück, AG Genetik, Barbarastr. 11, D-49076 Osnabrück, Germany. [§]These authors contributed equally to this work.

ABSTRACT Traditionally, the structural details of microbial cell walls are studied by thin-section electron microscopy, a technique that is very demanding and requires vacuum conditions, thus precluding live cell experiments. Here, we present a method integrating single-molecule atomic force microscopy (AFM) and protein design to measure cell wall thickness in a living yeast cell. The basic idea relies on the expression of His-tagged membrane sensors of increasing lengths in yeast and their subsequent specific detection at the cell surface using a modified AFM tip. After establishing the method on a wild-type strain, we demonstrate its potential by measuring changes in cell wall thickness within a few nanometers range, which result from (bio)chemical treatments or from mutations affecting the cell wall structure. The single molecular ruler method presented here not only avoids cell fixation artifacts but also provides new opportunities for studying the dynamics of microbial cell walls during growth, drug action, or enzymatic modification.

KEYWORDS: AFM · yeast cell wall · molecular rulers · sensors · single-molecule force microscopy

Microbial cells are surrounded by thick, mechanically strong cell walls which serve several key functions, such as resisting the internal turgor pressure of the cell, determining the shape of the organism, acting as a molecular sieve, protecting the cytoplasm from potentially harmful compounds in the outer environment, and harboring proteins for molecular recognition and cell adhesion.[1−3] In yeast, cell walls are made of a microfibrillar array of β-1−3 glucan and β-1−6 glucan chains, overlaid by mannoproteins, implying they are much stronger and stiffer than the glycocalyx of mammalian cells.[4−6] Yeast cell wall mannoproteins are highly glycosylated polypeptides (50−95% carbohydrate by weight), thus building up a proteoglycan layer.[6] Frequently, these structures are the target of specific antibiotics such as echinocandins, a group of glucan synthase inhibitors.[7] Moreover, the polysaccharide components interact with drugs such as Calcofluor white or Congo red, which trigger the cell wall integrity (CWI) signaling cascade and elicit cell wall synthesis and remodeling.[8,9] A deeper understanding of the functions of microbial cell walls requires a detailed knowledge of their morphological and structural features. Among these, cell wall thickness is a key parameter to monitor since it is modulated in response to environmental stimuli or drugs. For instance, in the milk yeast *Kluyveromyces lactis*, cell wall thickness varies in dependence of the carbon source used for growth.[10] Moreover, fungi from hypersaline environments are known to adapt to the high salinity by significantly increasing their cell wall thickness.[11] Likewise, the basidomycetes human pathogen *Cryptococcus neoformans* produces a secondary cell wall upon acidification of the medium.[12] In contrast, treatment of the human ascomycetes pathogen *Candida albicans* with different antifungal drugs has been shown to reduce cell wall thickness.[13,14] In fact, resistance of this pathogen to the antifungal drug Caspofungin, a glucan synthase inhibitor of the echinocandin family, is correlated to cell wall thickness.[15] In the nonpathogenic eukaryotic model yeast *Saccharomyces cerevisiae*, cell wall thickness varies dramatically depending on the metabolic conditions. For instance, oxidative stress caused by the addition of diamide leads to a strengthening of the cell wall.[16]

How exactly the yeast cell wall thickness is adjusted to external agents or mutations is still poorly understood, owing to the lack of suitable detection techniques in live cells. Apart from biochemical and biophysical determinations of cell wall compositions in ascomycete yeasts, thin-section transmission electron microscopy (TEM) is currently the only method available to determine cell wall thickness.[10,17,18] This approach is demanding and requires fixation

*Address correspondence to heinisch@biologie.uni-osnabrueck.de, yves.dufrene@uclouvain.be.

Received for review July 10, 2010 and accepted August 24, 2010.

Published online August 30, 2010. 10.1021/nn101598v

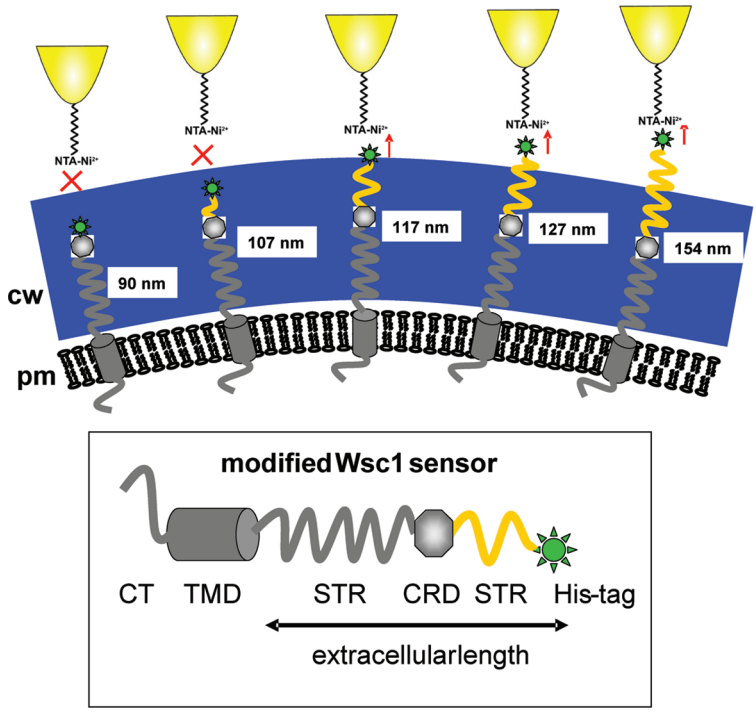

Figure 1. Use of molecular rulers to measure cell wall thickness. His-tagged and modified Wsc1 membrane sensors of various lengths were detected using AFM tips functionalized with Ni^{2+}-NTA groups. Only the sensors that were long enough to reach the surface were detected by the tip. The drawing below shows a modified Wsc1 sensor, with the cytoplasmic tail (CT), the transmembrane domain (TMD), the cysteine-rich domain (CRD), the serine/threonine-rich regions (STR) of variable length, and the terminal His-tag (in green); cw = cell wall, pm = plasma membrane.

and vacuum conditions, which impedes the investigation of cell wall thickness and dynamics in live cells. Here, we present a new method for measuring cell wall thickness in living *S. cerevisiae* cells, which integrates genetic manipulations and protein design with single-molecule atomic force microscopy (AFM).

RESULTS AND DISCUSSION

Our general strategy is based on the generation of a series of molecular rulers, that is, His-tagged and modified Wsc1 membrane sensors of various lengths, and their subsequent single-molecule detection using chemically modified AFM tips (Figure 1). The native Wsc1 sensor in yeast is located at the upper end of the CWI signaling pathway.[19] It is composed of a relatively short cytoplasmic tail, a single predicted transmembrane domain (TMD), a large external serine/threonine-rich region (STR), a cysteine-rich domain (CRD), presumably anchoring the sensor in the cell wall and necessary for clustering, and an amino terminal signal sequence for secretion.[20,21] Wsc1 is a peculiar protein in that it has a rod-like structure owing to its highly glycosylated STR region[22] and was recently shown to behave as a stiff nanospring.[23,24] Native Wsc1 sensors cannot reach the outermost cell surface since they extend a theoretical maximum of 80 nm above the plasma membrane, while the cell wall is thicker (approximately 105 nm for glucose-grown cells).[10] We therefore reasoned that the use of His-tagged elongated Wsc1 derivatives with a stepwise lengthening of a chimeric outer STR region from another sensor (Mid2) should force them to span the whole cell wall and reach the cell surface. Thus, they would be readily accessible to AFM tips terminated with Ni^{2+}-nitrilotriacetate (NTA) groups.[23,24] With this in mind, we designed a series of different sensors with a calculated extracellular length increasing from 90 to 154 nm (Table 1). These sensor length values are obtained by assuming a fully linear peptide chain and a length of a peptide bond of 0.36 nm. We expect that the shortest sensor to be detected under different growth conditions will provide an estimate of the cell wall thickness.

First, we established the technique on wild-type *S. cerevisiae* cells expressing Wsc1 sensors of increasing lengths (Figure 2 and Supporting Information Figure 1). For all strains, high-resolution images revealed a smooth and homogeneous surface (), consistent with earlier observations.[23] Spatially resolved force curves (1024 curves on 1 μm $\times$ 1 μm areas) were recorded across the cell surface using a Ni^{2+}-NTA tip to detect single sensors. Strains with long sensors ($\geq$117 nm) showed a substantial fraction of curves with specific adhesion events reflecting the detection of single sensors (Supporting Information Figure 1). As we previously showed, such specific curves show a first regime corresponding to the straightening of the extracellular polypeptide chain at very low force, followed by a linear region where force is directly proportional to extension, thus characteristic of a Hookean spring.[23] Nonlinear peaks were due to nonspecific adhesion to other

TABLE 1. Molecular Ruler Constructs Employed in This Work

yeast strain[a]	calculated extracellular length	integrated vector[b]	endocytosis signal[c]	3′ oligonucleotide used for truncation[d]
Y1	154	pJJH1159	wild type	none (pBH01)
Y17	142	pJJH1229	wild type	10.67: cgcgctcgagTTCGTCTACCAGCATTGCCTCC
Y16	137	pJJH1228	wild type	10.66: cgcgctcgagTTTCTCATCAGATTCAAGCACC
Y15	132	pJJH1227	wild type	10.65: cgcgctcgagTTCAGATTCTTCATCCTCCTC
Y2	127	pJJH1160	wild type	09.329: ggcgctcgagATCCGCAACTTCTGAATCATCG
Y3	122	pJJH1161	wild type	09.328: ggcgctcgagAACATCATCTTCATCCTCACTGTCG
Y4	117	pJJH1162	wild type	09.327: cgcgctcgagATCATCCCCATCAACAATCACTTC
Y5	112	pJJH1163	wild type	09.326: ggcgctcgagCACACCATCCACTACTGCCTATAATC
Y6	107	pJJH1164	wild type	09.325: ggcgctcgagCAGTATTATTAACGGTAAGACG
Y7	96	pJJH1167	wild type	09.324: cgcgctcgagTAAATCCAAAAGTTCGGGTC
Y8	90	pJJH1180	wild type	none (pBH02)
Y9	154	pJJH1214	NPF/AAI	none (pBH01)
Y20	142	pJJH1232	NPF/AAI	10.67: cgcgctcgagTTCGTCTACCAGCATTGCCTCC
Y19	137	pJJH1231	NPF/AAI	10.66: cgcgctcgagTTTCTCATCAGATTCAAGCACC
Y18	132	pJJH1230	NPF/AAI	10.65: cgcgctcgagTTCAGATTCTTCATCCTCCTC
Y10	127	pJJH1215	NPF/AAI	09.329: ggcgctcgagATCCGCAACTTCTGAATCATCG
Y11	122	pJJH1216	NPF/AAI	09.328: ggcgctcgagAACATCATCTTCATCCTCACTGTCG
Y12	117	pJJH1217	NPF/AAI	09.327: cgcgctcgagATCATCCCCATCAACAATCACTTC
Y13	112	pJJH1218	NPF/AAI	09.326: ggcgctcgagCACACCATCCACTACTGCCTATAATC
Y14	107	pJJH1219	NPF/AAI	09.325: ggcgctcgagCAGTATTATTAACGGTAAGACG

[a]All strains are derived from HOD48-1D (*wsc1::KlURA3 leu2−3,112*) and carry the sensor constructs integrated at the *leu2−3,112* locus as described in Methods. [b]All constructs are based on the integrative vector YIplac128 (*LEU2*). [c]The clathrin-dependent endocytosis signal in the cytoplasmic tail was either wild-type (NPFDD) or the first three amino acids altered to AAI, which abolishes sensor endocytosis.[26] [d]Each of these oligonucleotides was used in combination with 09.323 (5′-agaactcgagCTACTTACGGAAGAACGTGC-3′) to generate truncations by inverse PCR as described in Methods. Small letters indicate sequences which are not complementary to the template and were used to introduce a XhoI recognition site. The shortest and longest constructs were obtained from vectors described previously (pBH02 and pBH01, respectively[23]).

cell surface constituents and were therefore discarded (Supporting Information Figure 1).

The adhesion force histograms obtained from a total of 4096 curves (Figure 2) indicated that strains featuring sensors shorter than 112 nm showed essentially no specific adhesion events (only 0.3% of the force curves), thus no sensor detection. By contrast, strains with sensors with a length of at least 117 nm always showed a substantial fraction of specific adhesion events with a mean magnitude of 150−175 and 300−325 pN that we attribute primarily to monovalent and multivalent interactions between a single His_8 moiety with one and two NTA groups, respectively. However, we cannot exclude that some of the 300−325 pN forces also reflect the detection of two distinct His-tagged sensors.

The sensogram obtained by plotting the variation of the amount of detected sensors as a function of sensor length showed a sharp increase around 115 nm (Figure 3a). The sensogram clearly shows that shorter sensors (<110 nm) were never detected, indicating that they do not reach the surface, while longer ones (>120 nm) were detected with a rather constant value of 80 sensors/μm. From the derivative of this curve, we estimate the cell wall thickness to be 115 nm. This is approximately 10% higher than the 105 nm mean value determined with TEM.[10] This discrepancy between AFM and TEM measurements may have two origins. First, our calculated sensor lengths are based on the assumption of a linear peptide (273 amino acids in length for the extracellular part of the shortest sensor) and a length of a peptide bond of 0.36 nm, while proteins are usually not linear, but folded into complex tertiary structures. The nanospring behavior conferred by the STR region suggests that this region, which constitutes most of the extracellular part of the Wsc1 sensor, is indeed fairly linear and comes close to the calculated length.[23] However, the N-terminal CRD domain constituted by approximately 80 amino acids is expected to be folded and could account for the 10 nm difference. Second, the thinner cell wall measured by TEM could be an artifact caused by the invasive sample preparation procedure (*e.g.*, dehydration). By contrast, our AFM experiments enable one to directly probe wall thickness in native live cells. We estimate the precision of our method to be on the order of 5 nm based on the highly contrasted shape of the sensograms. This precision may still be improved by increasing the number of data points in each sensogram (*i.e.*, by increasing the number of wild-type and mutant strains carrying molecular rulers with further lengths variations, which is very demanding) and by decreasing the errors for each data point (thus increasing the number of force measurements, which is very challenging with the current technology). In the future, we expect that parallel and automated force measurements may help improve the throughput and precision of the method.

Having established the method on wild-type cells, we next analyzed whether the sensograms are sensitive to changes in cell wall thickness resulting from mu-

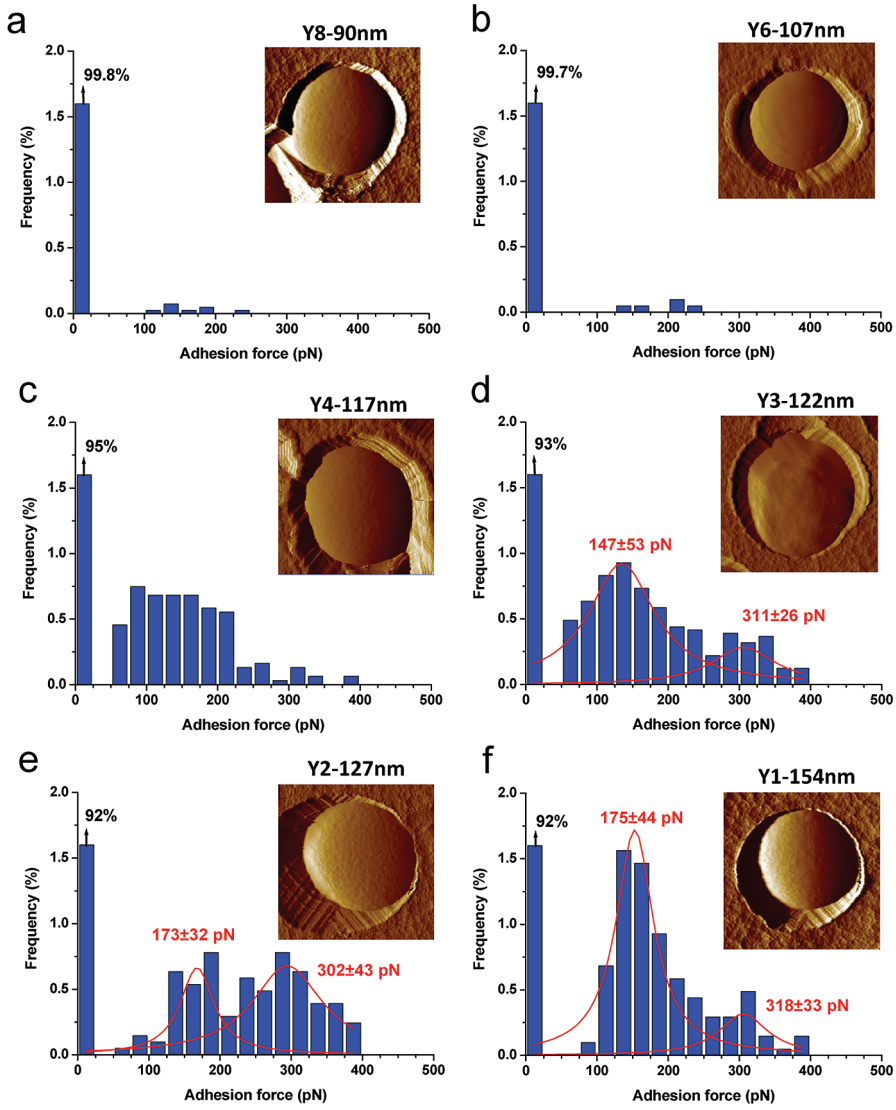

Figure 2. Sensor detection on wild-type cells. Adhesion force histograms (n = 4096 force curves) and AFM deflection images (insets, 5 μm × 5 μm) obtained on wild-type cells with Ni^{2+}-NTA tips in buffer solution (sodium acetate + sucrose 0.1 M, pH 4.75; note that these conditions have been shown previously to result in highly specific detection of His-tagged sensors at the yeast cell surface).[23] Strains expressing six membrane sensors of increasing extracellular length were employed: 90 nm (a), 107 nm (b), 117 nm (c), 122 nm (d), 127 nm (e), and 154 nm (f).

tations (Figure 3 and Supporting Information Figure 2). The native Wsc1 sensor is delivered to the plasma membrane by the classical secretion pathway and subsequently displays a high rate of internalization.[25] The latter is mediated by an endocytosis signal located within the cytoplasmic tail of the sensor, and mutation of this signal results in the construction of a much thicker cell wall.[26] If endocytosis of the sensor is inhibited, its concentration at the plasma membrane increases, presumably leading to a permanent signal generation, which in turn will trigger a more pronounced cell wall synthesis as compared to the wild-type. The biological importance of this process has recently been substantiated by the lower fitness of such Wsc1 endocytosis mutants in growth competition experiments with wild-type cells.[27] We therefore first investigated a strain carrying such mutant versions within the Wsc1 sensor ruler set ($Wsc1_{NPF/AAI}$). Similar to the strategy described above for the wild-type, the series of mutant sensors with increasing lengths was expressed from single-copy integrants at the *LEU2* locus in a *wsc1* deletion background and probed by AFM. As evident from Figure 3a, the $Wsc1_{NPF/AAI}$ mutation led to a dramatic change of the sensogram. Of all the sensors, only the two longest ones—with extracellular length of 142 and 154 nm—could be detected at the cell surface. This provides direct evidence that the mutant cell wall is much thicker, with an average *in vivo* thickness of approximately 140 nm. This is in good agreement with the hypothesis that the need for new cell wall biosynthesis is signaled through the Wsc1 sensor to the downstream CWI pathway components.[26]

We then explored whether the method can detect changes in cell wall thickness resulting from treatment

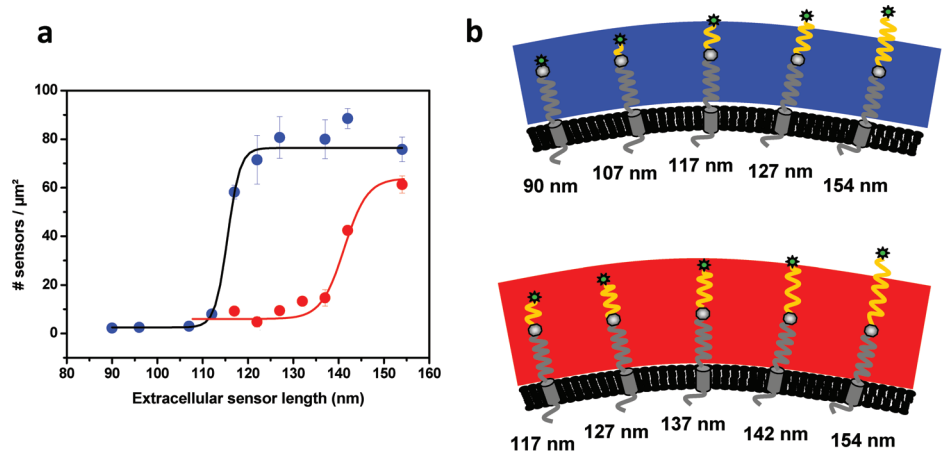

Figure 3. Sensograms are sensitive to changes in cell wall thickness resulting from mutations. Variation of the amount of detected sensors as a function of extracellular sensor length for wild-type cells (in blue) and for mutant cells expected to possess thicker cell walls (in red). Data represent the mean ± sem of the number of detected sensors, obtained from $n = 6144$ force curves from 6 maps (1 µm × 1 µm), using different tips and different cells. The drawing at the right emphasizes the major difference in cell wall thickness.

with Zymolyase or diamide (Figure 4). Diamide is known to cause oxidative stress, which results in the strengthening of the yeast cell wall.[16] On the other hand, Zymolyase is an enzyme mixture with high glucanase activity, which degrades cell wall polysaccharides (note that cell wall digesting enzymes have been extensively employed for the generation of spheroplasts, ever since the dawn of yeast molecular biology).[28,29] It is thus expected to rapidly produce thinner cell walls upon addition to yeast cells. As illustrated in Figure 4a, sensors with a length of 112 nm could still be detected in large amount on Zymolyase-treated cells, thus reflecting their thinner cell wall. Zymolyase-treated cells with short sensors (<112 nm) showed a very low number of sensors detected per µm², indicating that the enzymatic digestion essentially affected a 10 nm thick outer layer. Presumably, this moderate effect is due to the short incubation period with the enzyme mixture. Longer incubations will likely result in the production of too much debris interfering with the AFM tip, so that this cannot be tested due to experimental constraints. Nevertheless, we note that Zymolyase-treated cells with short sensors (<112 nm) showed a moderate sensor detectability (10 sensors/µm), an effect that we attribute to their heterogeneous cell wall structure. Consistent with this, AFM topographic images suggested that treated cells were rougher than native ones (Figure 4a).

In contrast to these results, even the longer sensors (up to 154 nm) could hardly be detected at the surface of diamide-treated cells, documenting thickening of the cell wall by more than 40 nm (Figure 4b). This agrees with images obtained from electron microscopy for cells grown under such conditions.[16] That the number of sensors at the surface of diamide-treated cells was strongly reduced (from ~80 to ~10 sensors/µm) but not completely abolished may be due to either a general heterogeneity in cell wall thickness caused by the

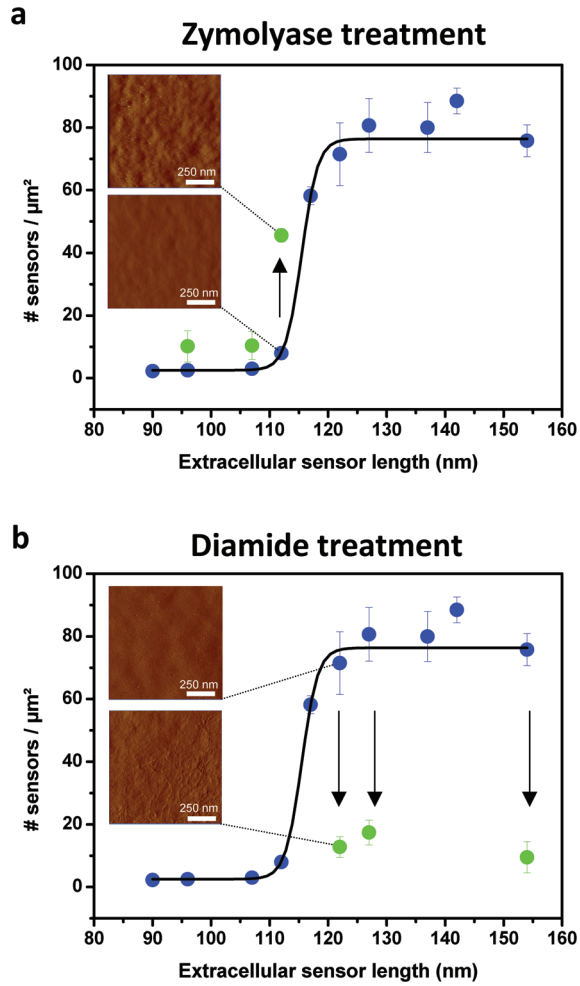

Figure 4. Sensograms reveal changes in cell wall thickness resulting from (bio)chemical treatments. Sensograms obtained for native wild-type cells (a and b; in blue), and for wild-type cells after Zymolyase treatment (a, in green) and after diamide treatment (b, in green). Data represent the mean ± sem of the number of detected sensors, obtained from $n = 6144$ force curves from 6 maps (1 µm × 1 µm), using different tips and different cells. Insets: high-resolution topographic images of the cells documenting a rougher surface after treatment.

oxidative stress exerted on the cell wall proteins or to an impact of diamide on sensor secretion. Supporting the former hypothesis, we found that the surface of treated cells was generally rougher than the one of untreated controls (Figure 4b).

CONCLUSION

Our experiments demonstrate that the use of His-tagged membrane sensors as molecular rulers combined with their detection by single-molecule AFM is a powerful platform for measuring cell wall thickness in live cells. The obtained sensograms are shown to be a valuable tool to detect thickness changes resulting from enzyme or drug treatment and are therefore expected to trigger a large number of investigations of biological and medical relevance. Obviously, other yeast surface sensors (*e.g.*, from the cell wall integrity or the high osmolarity signaling pathways) of *S. cerevisiae* and their relatives from other fungi are good candidates for future studies, with possible impacts on antifungal drug development.[7] Moreover, the study of mammalian sensors such as polycystin, which is related to hereditary polycystic kidney disease and shows some striking similarities to the Wsc1 sensor, could be of interest.[20] Compared to fluorescence methods traditionally used in cell wall research, our AFM approach is much more sensitive (single-molecule detection) and surface specific (no signal from the underlying layers). In fact, fluorescence microscopy showed that even the shortest His-tagged sensor constructs can be detected by using specific antibodies, indicating at least a partial permeability of the cell wall for the latter (unpublished results), which excludes this strategy for the determination of *in vivo* cell wall thickness.

METHODS

Media, Growth Conditions, Strains, and Genetic Manipulations. Media and standard procedures were applied as described.[30] The *S. cerevisiae* strains used in this work were exclusively derived from HOD48-1D (*MATa wsc1::KlURA3 ura3-52 leu2-3,112 his3-11,15*), which except for the mating type and the *wsc1* deletion is isogenic to the previously described strain HD56-5A.[31] All *WSC1* variants were subcloned into the vector YIplac128 and integrated at the *LEU2* locus of HOD48-1D by the one-step gene replacement method, selecting for leucine prototrophy.[32,33] Yeast transformation was performed by the freeze method.[34] Homologous recombination was triggered by digestion with BstEII prior to yeast transformation, and single-copy integration was confirmed by PCR using the oligonucleotide pair 06.3/06.4 (5′-GGCCGAGCGGTCTAAGGCGC-3′ and 5′-GTGGTGCCCTCCTCCTTGTC-3′) flanking the *LEU2* locus, in conjunction with the long-range high fidelity Taq polymerase kit from Fermentas. The $WSC1_{NPF/AAI}$ allele, carrying the mutated endocytosis signal at positions 344−346 in the deduced amino acid sequence, was obtained by *in vitro* mutagenesis as described elsewhere and introduced by several subcloning steps into YIplac128 prior to integration of the constructs at the *LEU2* locus (cloning details and plasmid sequences are available upon request).[27] In order to create the sensor ruler set, plasmid pJJH1147 was constructed. It contains the *Bam*HI/*Hin*dIII fragment encoding the chimeric 8xHis-Mid2-Wsc1 sensor from pBH01 subcloned into the respective sites of pUK1921;[23,35] pJJH1147 was then used as a template for inverse PCR reactions, with the oligonucleotide 09.323 (5′-AGAACTCGAGCTACTTACGGAAGAACGTGC-3′, which reads toward the 5′-end of the sensor construct starting from downstream of the 8xHis-tag coding sequence), in combination each with one of the oligonucleotides 09.324−09.329 and 10.65−10.67 to consecutively shorten the protein coding sequence, as listed in Table 1. All oligonucleotides contained an in-frame XhoI recognition sequence at their 5′-end, which allowed for digestion of the PCR products and their circularization by T4-DNA ligase. After amplification in *E. coli*, the resulting clones were sequenced to eliminate candidates with grave PCR errors within the sensor coding sequence and subcloned into YIplac128.

For AFM studies, transformants were cultured in leucine-free synthetic media as follows. Two or three colonies from the solid medium plate used as inoculum were transferred into culture medium. Cells were agitated overnight at 30 °C, grown up to the late logarithmic phase, and harvested by centrifugation. They were washed three times with sodium acetate buffer and resuspended in 10 mL buffer to a concentration of $\sim 10^6$ cells/mL. For some experiments, cells were pretreated with diamide (Sigma). To this end, 500 μL of a 10 mM diamide solution was added into leucine-free synthetic media. For Zymolyase experiments, 50 μL of a Zymolyase solution (Sigma, 0.3 mg/mL, supplied as "Lyticase" from *Athrobacter luteus*) was injected into the AFM liquid cell.

Atomic Force Microscopy. AFM measurements were performed in buffered solutions (sodium acetate +0.1 M sucrose, pH 4.75) using a Nanoscope IV Multimode AFM (Veeco Metrology Group). Sharpened silicon nitride cantilevers (MSCT, Veeco) and gold-coated cantilevers (OMCL-TR4, Olympus Ltd., Tokyo, Japan) were used for imaging and force measurements, respectively. Gold-coated cantilevers were cleaned for 15 min by UV and ozone treatment, rinsed with ethanol, dried with a gentle nitrogen flow, immersed overnight in ethanol containing 0.01 mM of NTA-terminated alkanethiols (ProChimia, Poland), rinsed with ethanol, further immersed in a 40 mM aqueous solution of $NiSO_4$ (pH 7.2) for 1 h, and then finally rinsed with buffer. Cells were immobilized by mechanical trapping into porous polycarbonate membranes with 3 μm pore size (Millipore). The pore diameter was modified to match the cell diameter by etching overnight in 10 mL of 5 M NaOH (Sigma) at room temperature.[36] Membranes were then rinsed several times in Milli-Q water. After filtering a concentrated cell suspension, the filter was gently rinsed with buffer, carefully cut (1 cm × 1 cm) and attached to a steel sample puck (Veeco Metrology Group) using a small piece of double-face adhesive tape, and the mounted sample was transferred into the AFM liquid cell while avoiding dewetting. We first imaged the topography of single yeast cells by engaging a silicon nitride tip and scanning the sample in contact mode. To detect His-tagged sensors by force spectroscopy, the tip was changed with a Ni^{2+}-NTA-gold tip and then re-engaged on the cell of interest. The spring constants of the Ni^{2+}-NTA-gold cantilevers were measured using the thermal noise method (Picoforce, Veeco Metrology Group), yielding values ranging from 0.02 to 0.028 N/m. Unless otherwise specified, all force measurements were performed using a constant approach and retraction speed of 1500 nm/s, and with an interaction time of 500 ms.

Acknowledgment. This work was supported by the National Foundation for Scientific Research (FNRS), the Université catholique de Louvain (Fonds Spéciaux de Recherche), the Région wallonne, the Federal Office for Scientific, Technical and Cultural Affairs (Interuniversity Poles of Attraction Programme), and the Research Department of the Communauté française de Belgique (Concerted Research Action). Y.F.D. is Senior Research Associate at the FNRS. Work at the University of Osnabrück was

funded by the Deutsche Forschungsgemeinschaft (DFG) within the framework of the SFB431.

Supporting Information Available: Specificity of sensor detection, representative specific and nonspecific force curves using the Ni^{2+}-NTA tips are given in Supplementary Figure 1. Supplementary Figure 2 shows the adhesion force histograms and AFM images obtained on mutant cells with thicker cell walls and carrying different sensor constructs. This material is available free of charge *via* the Internet at http://pubs.acs.org.

REFERENCES AND NOTES

1. Beveridge, T. J.; Graham, L. L. Surface Layers of Bacteria. *Microbiol. Rev.* **1991**, *55*, 684–705.
2. Margolin, W. Sculpting the Bacterial Cell. *Curr. Biol.* **2009**, *19*, R812–822.
3. Nather, K.; Munro, C. A. Generating Cell Surface Diversity in *Candida albicans* and Other Fungal Pathogens. *FEMS Microbiol. Lett.* **2008**, *285*, 137–145.
4. Fleet, G. H. *Yeast Organelles: Cell Walls*; Academic Press: London, 1991; Vol. 4, pp 199−277.
5. Lesage, G.; Bussey, H. Cell Wall Assembly in *Saccharomyces cerevisiae*. *Microbiol. Mol. Biol. Rev.* **2006**, *70*, 317–343.
6. Lipke, P. N.; Ovalle, R. Cell Wall Architecture in Yeast: New Structure and New Challenges. *J. Bacteriol.* **1998**, *180*, 3735–3740.
7. Heinisch, J. J. Baker's Yeast as a Tool for the Development of Antifungal Drugs Which Target Cell Integrity—An Update. *Expert Opin. Drug Discovery* **2008**, *3*, 931–943.
8. Roncero, C.; Duran, A. Effect of Calcofluor White and Congo Red on Fungal Wall Morphogenesis: *In Vivo* Activation of Chitin Polymerization. *J. Bacteriol.* **1985**, *163*, 1180–1185.
9. Levin, D. E. Cell Wall Integrity Signaling in *Saccharomyces cerevisiae*. *Microbiol. Mol. Biol. Rev.* **2005**, *69*, 262–291.
10. Backhaus, K.; Heilmann, C. J.; Sorgo, A. G.; Purschke, G.; de Koster, C. G.; Klis, F. M.; Heinisch, J. J. A Systematic Study of the Cell Wall Composition of *Kluyveromyces lactis*. *Yeast* **2010**, *27*, 647−660.
11. Kralj Kuncic, M.; Kogej, T.; Drobne, D.; Gunde-Cimerman, N. Morphological Response of the Halophilic Fungal Genus *Wallemia* to High Salinity. *Appl. Environ. Microbiol.* , *76*, 329–337.
12. Farkas, V.; Takeo, K.; Macekova, D.; Ohkusu, M.; Yoshida, S.; Sipiczki, M. Secondary Cell Wall Formation in *Cryptococcus neoformans* as a Rescue Mechanism Against Acid-Induced Autolysis. *FEMS Yeast Res.* **2009**, *9*, 311–320.
13. Braga-Silva, L. A.; Mogami, S. S.; Valle, R. S.; Silva-Neto, I. D.; Santos, A. L. Multiple Effects of Amprenavir Against *Candida albicans*. *FEMS Yeast Res.* , *10*, 221–224.
14. Nishiyama, Y.; Uchida, K.; Yamaguchi, H. Morphological Changes of *Candida albicans* Induced by Micafungin (FK463), a Water-Soluble Echinocandin-like Lipopeptide. *J. Electron Microsc. (Tokyo)* **2002**, *51*, 247–255.
15. Plaine, A.; Walker, L.; Da Costa, G.; Mora-Montes, H. M.; McKinnon, A.; Gow, N. A.; Gaillardin, C.; Munro, C. A.; Richard, M. L. Functional Analysis of *Candida albicans* GPI-Anchored Proteins: Roles in Cell Wall Integrity and Caspofungin Sensitivity. *Fungal Genet. Biol.* **2008**, *45*, 1404–1414.
16. Vilella, F.; Herrero, E.; Torres, J.; de la Torre-Ruiz, M. A. Pkc1 and the Upstream Elements of the Cell Integrity Pathway in *Saccharomyces cerevisiae*, Rom2 and Mtl1, Are Required for Cellular Responses to Oxidative Stress. *J. Biol. Chem.* **2005**, *280*, 9149–9159.
17. Klis, F. M.; Brul, S.; deGroot, P. W. J.; Covalently Linked Wall Proteins in Ascomycetous Fungi. *Yeast* **2010**, *27*, 489−493.
18. Osumi, M. The Ultrastructure of Yeast: Cell Wall Structure and Formation. *Micron* **1998**, *29*, 207–233.
19. Rodicio, R.; Heinisch, J. J. Together We Are Strong: Cell Wall Integrity Sensors in Yeasts. *Yeast* **2010**, *27*, 531−540.
20. Heinisch, J. J.; Dufrene, Y. F. Is There Anyone out There? Single Molecule Atomic Force Microscopy Meets Yeast Genetics to Study Sensor Functions. *Integr. Biol.* **2010**, DOI: 10.1039/c1030ib00012d.
21. Heinisch, J. J.; Dupres, V.; Wilk, S.; Jendretzki, A.; Dufrene, Y. F. Single-Molecule Atomic Force Microscopy Reveals Clustering of the Yeast Plasma-Membrane Sensor Wsc1. *PLoS One* **2010**, *5*, e11104.
22. Philip, B.; Levin, D. E. Wsc1 and Mid2 Are Cell Surface Sensors for Cell Wall Integrity Signaling That Act Through Rom2, A Guanine Nucleotide Exchange Factor for Rho1. *Mol. Cell. Biol.* **2001**, *21*, 271–280.
23. Dupres, V.; Alsteens, D.; Wilk, S.; Hansen, B.; Heinisch, J. J.; Dufrene, Y. F. The Yeast Wsc1 Cell Surface Sensor Behaves Like a Nanospring *In Vivo*. *Nat. Chem. Biol.* **2009**, *5*, 857–862.
24. Heinisch, J. J.; Dupres, V.; Alsteens, D.; Dufrene, Y. F. Measurement of the Mechanical Behavior of Yeast Membrane Sensors Using Single-Molecule Atomic Force Microscopy. *Nat. Protocols* **2010**, *5*, 670–677.
25. Straede, A.; Heinisch, J. J. Functional Analyses of the Extra- and Intracellular Domains of the Yeast Cell Wall Integrity Sensors Mid2 and Wsc1. *FEBS Lett.* **2007**, *581*, 4495–4500.
26. Piao, H. L.; Machado, I. M.; Payne, G. S. NPFXD-Mediated Endocytosis is Required for Polarity and Function of a Yeast Cell Wall Stress Sensor. *Mol. Biol. Cell* **2007**, *18*, 57–65.
27. Wilk, S.; Wittland, J.; Thywissen, A.; SchmitzH. P.; Heinisch, J. J. A Block of Endocytosis of the Yeast Cell Wall Integrity Sensors Wsc1 and Wsc2 Results in a Reduced Fitness *In Vivo*. *Molec. Genet. Genom.* **2010**, *284*, 217−229.
28. Beggs, J. D. Transformation of Yeast By a Replicating Hybrid Plasmid. *Nature* **1978**, *275*, 104–109.
29. Struhl, K.; Stinchcomb, D. T.; Scherer, S.; Davis, R. W. High-Frequency Transformation of Yeast: Autonomous Replication of Hybrid DNA Molecules. *Proc. Natl. Acad. Sci. U.S.A.* **1979**, *76*, 1035–1039.
30. Sherman, F.; Fink, G. R.; Hicks, J. B. *Laboratory Course Manual for Methods in Yeast Genetics*; Cold Spring Harbor Laboratory: New York, 1986.
31. Arvanitidis, A.; Heinisch, J. J. Studies on the Function of Yeast Phosphofructokinase Subunits By *In Vitro* Mutagenesis. *J. Biol. Chem.* **1994**, *269*, 8911–8918.
32. Gietz, R. D.; Sugino, A. New Yeast−*Escherichia coli* Shuttle Vectors Constructed with *In Vitro* Mutagenized Yeast Genes Lacking Six-Base Pair Restriction Sites. *Gene* **1988**, *74*, 527–534.
33. Rothstein, R. Targeting, Disruption, Replacement, and Allele Rescue: Integrative DNA Transformation in Yeast. *Methods Enzymol.* **1991**, *194*, 281–301.
34. Klebe, R. J.; Harriss, J. V.; Sharp, Z. D.; Douglas, M. G. A General Method for Polyethylene-Glycol-Induced Genetic Transformation of Bacteria and Yeast. *Gene* **1983**, *25*, 333–341.
35. Heinisch, J. J. *PFK2, ISP42, ERG2* and *RAD14* Are Located on the Right Arm of Chromosome XIII. *Yeast* **1993**, *9*, 1103–1105.
36. Turner, R. D.; Thomson, N. H.; Kirkham, J.; Devine, D. Improvement of the Pore Trapping Method to Immobilize Vital Coccoid Bacteria for High-Resolution AFM: A Study of *Staphylococcus aureus*. *J. Microsc.* **2010**, *238*, 102–110.